SCIENTIFIC REPORTS

OPEN

SUBJECT AREAS:
TISSUE ENGINEERING
MEDICAL RESEARCH
REGENERATIVE MEDICINE

Received
19 February 2014

Accepted
18 July 2014

Published
13 August 2014

Correspondence and requests for materials should be addressed to T.T. (t-tsuji@rs.noda.tus.ac.jp)

* These authors contributed equally to this work.

† Current address: Department of Oral Rehabilitation and Regenerative Medicine, Graduate School of Medicine, Dentistry and Pharmaceutical Sciences, Okayama University, Okayama, 700-8525, JAPAN.

§ Current address: RIKEN Center for Developmental Biology, Kobe, Hyogo, 650-0047, JAPAN.

Functional tooth restoration by next-generation bio-hybrid implant as a bio-hybrid artificial organ replacement therapy

Masamitsu Oshima[1*†], Kaoru Inoue[2,3*], Kei Nakajima[2,4], Tetsuhiko Tachikawa[5], Hiromichi Yamazaki[2], Tomohide Isobe[5], Ayaka Sugawara[2], Miho Ogawa[1,6], Chie Tanaka[2], Masahiro Saito[2], Shohei Kasugai[7], Teruko Takano-Yamamoto[3], Takashi Inoue[4], Katsunari Tezuka[1,6], Takuo Kuboki[8], Akira Yamaguchi[9] & Takashi Tsuji[1,2,6§]

[1]Research Institute for Science and Technology, Tokyo University of Science, Noda, Chiba, 278-8510, JAPAN, [2]Department of Biological Science and Technology, Graduate School of Industrial Science and Technology, Tokyo University of Science, Noda, Chiba, 278-8510, JAPAN, [3]Division of Orthodontics and Dentofacial Orthopedics, Graduate School of Dentistry, Tohoku University, Sendai, Miyagi, 980-8575, JAPAN, [4]Department of Clinical Pathophysiology, Tokyo Dental College, Chiba-shi, Chiba, 261-8502, JAPAN, [5]Department of Oral Pathology, Showa University School of Dentistry, Shinagawa-ku, Tokyo, 145-8515, JAPAN, [6]Organ Technologies Inc., Tokyo, 108-0074, JAPAN, [7]Section of Oral Implantology and Regenerative Dental Medicine, Graduate School of Tokyo Medical and Dental University, Bunkyo-ku, Tokyo 113-8549, JAPAN, [8]Department of Oral Rehabilitation and Regenerative Medicine, Graduate School of Medicine, Dentistry and Pharmaceutical Sciences, Okayama University, Okayama, 700-8525, JAPAN, [9]Section of Oral Pathology, Department of Oral Restitution, Graduate School of Tokyo Medical and Dental University, Bunkyo-ku, Tokyo 113-8549, JAPAN.

Bio-hybrid artificial organs are an attractive concept to restore organ function through precise biological cooperation with surrounding tissues *in vivo*. However, in bio-hybrid artificial organs, an artificial organ with fibrous connective tissues, including muscles, tendons and ligaments, has not been developed. Here, we have enveloped with embryonic dental follicle tissue around a HA-coated dental implant, and transplanted into the lower first molar region of a murine tooth-loss model. We successfully developed a novel fibrous connected tooth implant using a HA-coated dental implant and dental follicle stem cells as a bio-hybrid organ. This bio-hybrid implant restored physiological functions, including bone remodelling, regeneration of severe bone-defect and responsiveness to noxious stimuli, through regeneration with periodontal tissues, such as periodontal ligament and cementum. Thus, this study represents the potential for a next-generation bio-hybrid implant for tooth loss as a future bio-hybrid artificial organ replacement therapy.

Organ functions are achieved via biological cooperation with surrounding tissues and other organs[1]. Alternative therapies using artificial organs represent an approach to partially support organ function *in vivo*, but they presently are not able to entirely replace organ function[2]. A bio-hybrid artificial organ is an attractive concept to restore organ function through precise biological cooperation with surrounding tissues *in vivo*[2,3]. In the blood circulatory system, physical functions including pumping and filtration have been conventionally substituted using ventricular assist devices and *ex vivo* dialysis systems for heart and kidney failure, respectively[2,4]. In sensory organ dysfunction, bio-hybrid artificial eyes and cochlear implants have aided in the functional restoration of visual impairment and hearing loss, respectively, via afferent neural transmission to the central nervous system (CNS)[5,6]. A bio-hybrid artificial arm that is operated by efferent neural control from the CNS has also been developed as a bio-hybrid organ for irreversible arm loss[7]. In the skeletal system, artificial joints have achieved osseo-integration with bone tissue and have contributed to the support of mechanical loading[8]. Fibrous connective tissues, including muscles, tendons and ligaments, play important roles in exerting biological organ functions, such as tight connectivity, proper flexibility, mobility and resistance against mechanical stimulations[8]. However, in bio-hybrid artificial organs, a fibrous connective artificial organ has not been structurally and functionally established, and further technological improvements are required to achieve fully functional cooperation between an artificial organ and the surrounding tissues[3,8].

Organs, including eyes, joints and teeth, are connected to surrounding tissues via fibrous connective tissues so that they can efficiently perform their biological functions[9]. The periodontal ligament (PDL), which is developed from the dental follicle in tooth germ, is one of the fibrous connective tissues between the tooth-root and the jawbone[10]. The PDL plays essential physiological roles in the absorption of occlusal loading and orthodontic tooth movement accompanied by bone remodelling, and it contributes to the functional cooperation among the teeth, masticatory muscles and temporomandibular joint under the control of the CNS[11,12]. After tooth loss as a result of dental disorders such as caries, periodontal disease or injury, tooth restoration is traditionally performed by replacement with artificial material, such as fixed or removable dentures[13,14]. In addition, an osseo-integrated dental implant that directly connects with the alveolar bone independent of the PDL has been widely applied for the rehabilitation of tooth loss[15,16]. However, current dental implants are not adaptable to patients in the process of jawbone growth and to those patients with severe bone defects[11,16]. It has been therefore expected to develop a fully functional dental implant that satisfies physiological and functional requirements, including bone remodelling, cooperation with the maxillofacial region and sensing of noxious stimulation through connection with a bioengineered PDL as a fibrous connected bio-hybrid organ[17,18].

Regenerative medicine, which developed due to our understanding of embryonic development, stem cell biology and tissue engineering technologies, is an attractive concept to restore organ function[19–21]. Stem cell transplantation therapies have been developed to restore the partial loss of organ functions by replacing hematopoietic stem cells in leukaemia[22] and neural stem cells in spinal injury[23]. Bioengineered two-dimensional tissues have also been used to efficiently repair diseases such as severe burn, corneal injury and myocardial infarction[24,25]. Recently, advances in 3D stem cell manipulation and culturing have been used to understand cell differentiation, cell assembly and multicellular tissue organisation, providing capabilities beyond those of 2D cell cultures[19,26]. It is expected to further develop medical innovations using stem cells that can regenerate for severe disorders such as extensive tissue injury or organ dysfunction[19,26]. To develop a novel bio-hybrid artificial organ that can perform all of the biological organ functions *in vivo*, regenerative medicine technologies using stem cells and culture could improve the functions of several artificial organs[27,28].

In this study, we developed a novel fibrous connected tooth implant using a dental implant and dental follicle stem cells as a bio-hybrid organ. The bio-hybrid implant restored physiological functions, including bone remodelling, regeneration of critical bone-defect and responsiveness to noxious stimulations, through regeneration with periodontal tissues, such as cementum, PDL and alveolar bone. Thus, this study highlights the potential of a next-generation bio-hybrid implant for treating tooth loss as a future bio-hybrid artificial organ replacement therapy.

Results

Periodontal tissue formation on an artificial material using dental follicle tissue. To identify cell sources to regenerate periodontal tissue on an artificial material, a particle of hydroxyapatite (HA), we first investigated whether dental tissues isolated from several tooth developmental stages have the potential to form correct periodontal tissues, including cementum, PDL and alveolar bone, on the HA particle in a subrenal capsule *in vivo* (Supplementary Fig. 1a, b and Fig. 1a). The transplantation of a dental mesenchymal tissue isolated from the tooth germ at embryonic day (ED) 14.5 formed bone around the HA particle. Incomplete periodontal tissues with bone and PDL-like fibres, but not cementum, formed around the HA particle after transplantation with dental follicle tissues isolated from tooth germ at postnatal day (PD) 7 and PDL isolated from a mature tooth at PD35 (Supplementary Fig. 1c). Only dental follicle tissue at ED18.5 was able to form the entirely correct periodontal tissue, including cementum, PDL and alveolar bone, on the HA surface. We further analysed the gene expression patterns associated with periodontal tissue during the each developmental stage (Supplementary Fig. 2a). A multi-layered gene expression profile, including *F-spondin*, *Periostin* and *Osteocalcin*, which are the markers for cementoblasts, PDL cells and osteoblasts[29], respectively, was observed in the inner, middle and outer layers, respectively, of dental follicle tissue at ED18.5; the only stage that was able to generate the correct periodontal structure compared with dental tissues from other developmental stages[30] (Fig. 1b, c and Supplementary Fig. 2a, b). These results indicated that ED18.5 tooth germ-derived dental follicle tissue (ED18.5-DF) is a suitable cell source to generate periodontal tissues, including cementum, PDL and alveolar bone.

Transplantation of a bio-hybrid implant into a tooth loss region. We next investigated whether a dental titanium implant in combination with ED18.5-DF could serve as a bio-hybrid implant with periodontal tissue after engraftment in a tooth loss-region in the adult mouse oral environment (Fig. 1a). To adhere the ED18.5-DF to the implant and promote cementum formation, HA sputter deposition was performed to impart biocompatibility and osteoinductivity[31] and to form a rough structure on the titanium implant surface[32] (Fig. 1d). The implant was enveloped with ED18.5-DF in the correct orientation of the multi-layered DF (Fig. 1e) and transplanted into the lower first molar region of a murine tooth-loss model[33] (Supplementary Fig. 3a, b). Micro-CT and histochemical analyses revealed alveolar bone formation around the implant, referred to osseo-integration, at 30 days after transplantation of the HA-coated implant alone (Fig. 1f, g). In contrast, in the engrafted implant with ED18.5-DF (bio-hybrid implant), the periodontal ligament space and correct periodontal tissue structure consisting of cementum, PDL and alveolar bone were observed on the HA-coated implant (Fig. 1f, g). The PDL fibre structure of the engrafted bio-hybrid implant, which was comprised of transverse collagen fibres and longitudinal elastin fibres, was equivalent to a natural molar tooth (Fig. 1g and Supplementary Fig. 4a, b). The width of the formed PDL around the bio-hybrid implant was clearly detected and comparable to that of a natural tooth (Fig. 1h). After transplantation of bio-hybrid implant with green fluorescence protein (GFP)-transgenic mouse-derived ED18.5-DF, green fluorescence was clearly detectable around the implant at 30 days after transplantation (Fig. 1i and Supplementary Fig. 4c). These results indicate that the HA-coated implant with ED18.5-DF was able to generate periodontal tissues and could be a bio-hybrid implant as a fibrous connective artificial organ.

Structural analysis of the periodontal tissue in the bio-hybrid implant. Periodontal tissue plays important roles in cooperating with the maxillofacial region through the connection with fibre structures in the PDL[11,12]. Thus, we used electro mapping to analyse the ultrastructure of the periodontal ligament on the implant with ED18.5-DF and bone matrices. Although the osseo-integrated implant directly connected to the surrounding alveolar bone, the engrafted bio-hybrid implant showed that the PDL fibre was connected to the implant surface by scanning electron microscopy (SEM) analysis (Fig. 2a). Transmission electron microscopy (TEM) analysis revealed the correct cementum formation on the surface of the bio-hybrid implant and an invasion of Sharpey's fibre into the cementum of the bio-hybrid implant (Fig. 2b, c). Electron probe micro analysis revealed that in the region of the periodontal tissues of both a natural tooth and a bio-hybrid implant, specific elements of hard tissue, such as calcium (Ca; red) and phosphorus (P; green), were detected at high concentrations in the region of cementum and alveolar bone, but not in the PDL region (EPMA; Fig. 2d, e and Supplementary Fig. 5). These results

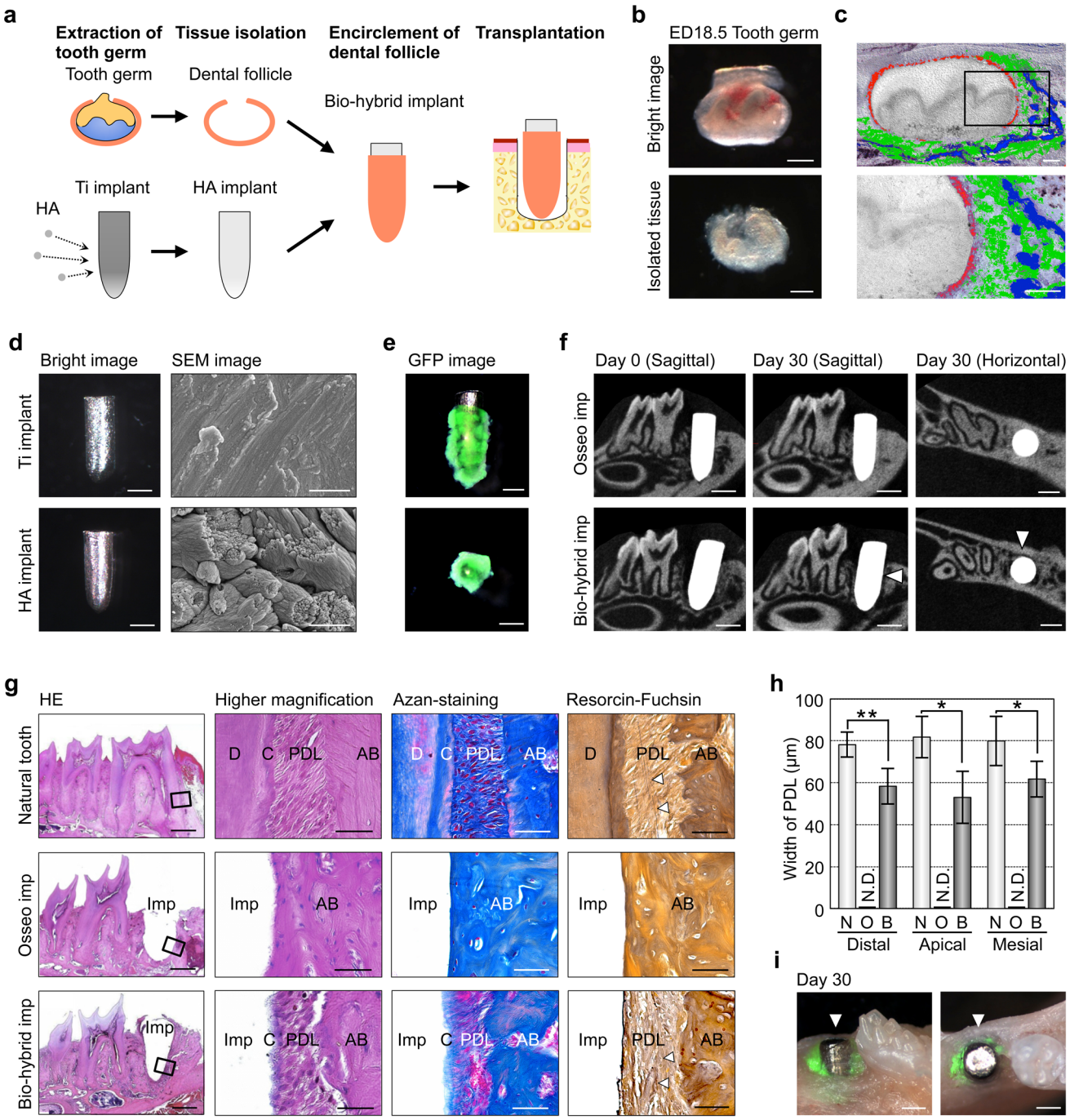

Figure 1 | Engraftment of a bio-hybrid implant in a tooth loss model. (a) Schematic representation of the generative technology of bio-hybrid implant. (Drawings by C.T.). (b) Photographs of ED18.5 tooth germ (*upper*) and isolated dental follicle tissue (*lower*). Scale bar, 100 μm. (c) Layer arrangement indicated by *in situ* hybridisation analysis for the expression patterns of *F-spondin* (red), *Periostin* (green) and *Osteocalcin* (blue) in ED18.5 dental follicle tissue. Scale bar, 100 μm. (d) Photographs (*left*) and surface analysis (*right*) of titanium implant and HA implant using SEM. Scale bar, 500 μm and 1.0 μm in the photographs and SEM images, respectively. (e) Merged images of a bio-hybrid dental implant using ED18.5 dental follicles isolated from GFP transgenic mice (*upper*, sagittal view; *lower*, horizontal view). Scale bar, 500 μm. (f) Micro-CT images of an osseo-integrated implant and a bio-hybrid implant to in sagittal section (*left, centre*) and horizontal section (*right*) at transplantation period of Day 0 and Day 30. Bio-hybrid implant images were observed in the periodontal ligament space (arrowhead). Scale bar, 500 μm. (g) Histological analysis of a natural tooth (*upper*), an engrafted osseo-integrated implant (*middle*) and an engrafted bio-hybrid implant (*lower*) at 30 days post-transplantation was performed. HE, Azan, and Resorcin-Fuschin staining are shown. Scale bar, 500 μm in the lower magnification (*left column*) and 50 μm in the higher magnification (*centre-left, centre-right and right column*). D, dentin; C, cementum; AB, alveolar bone; PDL, periodontal ligament; Imp, implant. (h) Measurement of the width of periodontal ligament area. The periodontal ligament was not detected in osseo-integrated implants at 30 days post-transplantation. N, natural tooth; O, osseo-integrated implant; B, bio-hybrid implant; N.D., Not detected. Error bars represent the standard deviation ($n = 5$). *$p < 0.05$, **$p < 0.01$ (Mann-Whitney U-test). (i) Photograph of a bio-hybrid implant using ED18.5 dental follicles isolated from GFP transgenic mice at 30 days post-transplantation. Arrowhead, bio-hybrid implant. Scale bar, 500 μm.

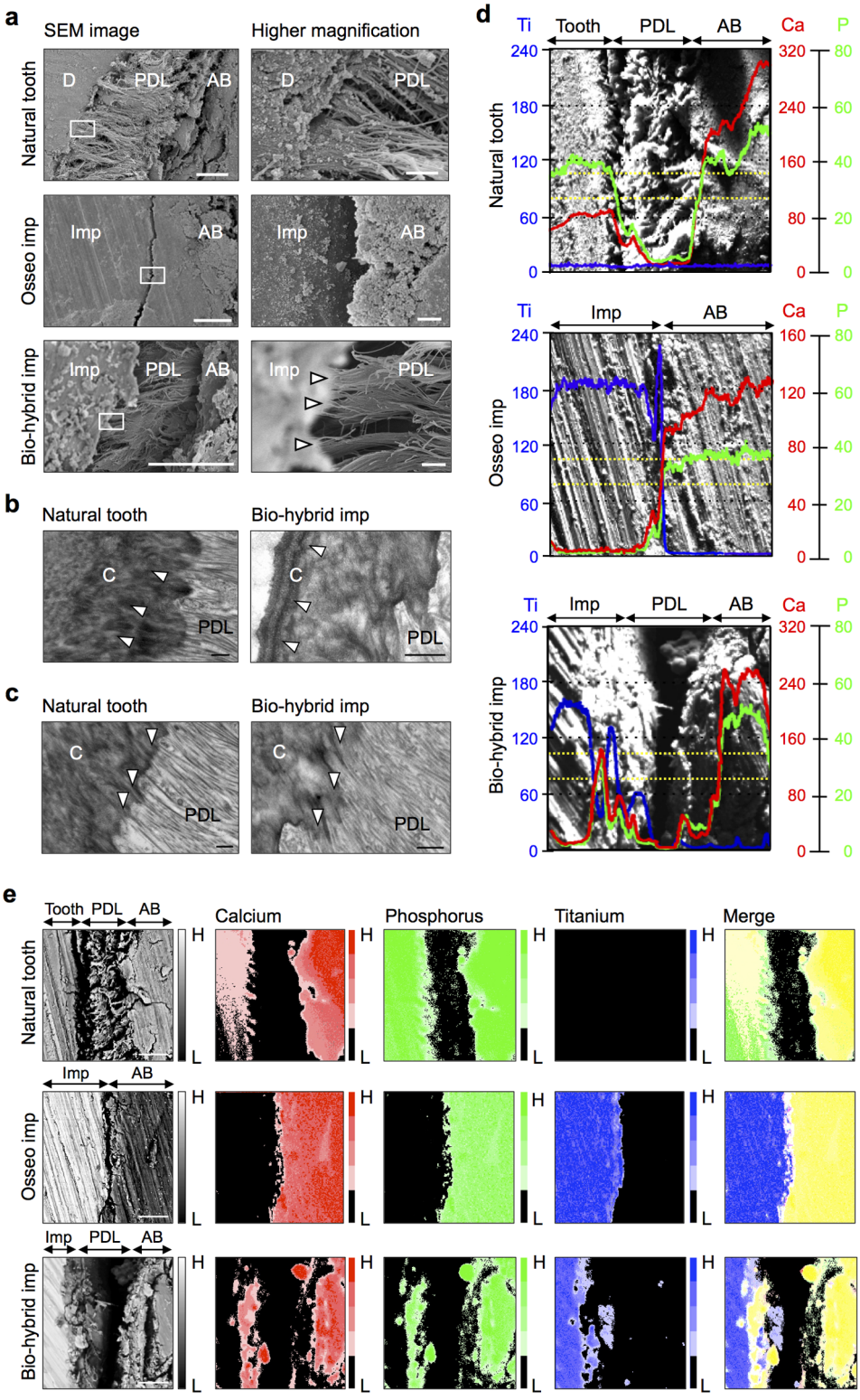

Figure 2 | Structural analyses of a periodontal tissue in the bio-hybrid implant. (a) Scanning electron microscopic (SEM) images of natural tooth (*upper*), the engrafted osseo-integrated implant (*middle*) and the engrafted bio-hybrid implant (*lower*) at 30 days post transplantation was performed. Scale bar, 20 μm and 1.0 μm in the lower and higher magnification, respectively. D, dentin; AB, alveolar bone; PDL, periodontal ligament; Imp, implant. (b and c) Transmission electron microscopic (TEM) observation of a natural tooth (*left*) and the engrafted bio-hybrid implant (*right*). Formation of lamellar cementum (b, arrowhead) and invasion of Sharpey's fibres into the cementum (c, arrowhead). Scale bar, 500 nm. C, cementum; PDL, periodontal ligament. (d) Amounts of calcium (Ca, red), phosphorus (P, green), and titanium (Ti, blue) in a natural tooth (*top*), the engrafted osseo-integrated implant (*middle*) and the engrafted bio-hybrid implant (*bottom*), as determined by SEM. The amounts of elements were measured in the area between dotted lines. AB, alveolar bone; PDL, periodontal ligament; Imp, implant. (e) Elemental mapping superposition of the natural tooth (*top*), osseo-integrated implant (*middle*) and bio-hybrid implant (*bottom*). Calcium (Ca, red), phosphorus (P, green), titanium (Ti, blue) and merged images are shown. AB, alveolar bone; PDL, periodontal ligament; Imp, implant.

demonstrated that the engrafted bio-hybrid implant formed the correct periodontal tissue architecture on the implant surface and the proper fibrous structural connections were formed.

Functional analysis of the periodontal ligament and nerve fibres of the bio-hybrid implant. It has been postulated that a fibrous connective artificial implant functioning as a bio-hybrid organ could be achieved by fulfilling critical functions in the oral environment, such as the cooperation of the bio-hybrid implant with the oral and maxillofacial regions through the PDL[34]. Therefore, we investigated whether an engrafted bio-hybrid implant could restore physiological periodontal functions, specifically the response to mechanical stress and the ability to perceive noxious stimulations *in vivo*. When we analysed the orthodontic movement using a mechanical force in an experimental tooth movement model, the bio-hybrid implant moved in a similar manner to natural teeth in response to orthodontic force (Fig. 3a, b). During experimental tooth movement, colony-stimulating factor-1 (*Csf-1*) mRNA-positive cells, which were used as a marker of osteoclastogenesis, and osteocalcin (*Ocn*) mRNA-positive osteoblasts were observed on the compression and tension sides, respectively[33,35,36] (Fig. 3c). These results demonstrate that the PDL of the bio-hybrid implant successfully mediates bone remodelling via the proper localisation of osteoclasts and osteoblasts in response to mechanical stress and that the implant represents a fibrous connective bio-hybrid implant.

The ability to perceive noxious stimulation, including mechanical stress and pain, are important for proper tooth function[34]. Trigeminal ganglional neurons, which innervate the pulp and PDL, can respond to these stimuli and transduce signals to the CNS. Anti-neurofilament (NF)-immunoreactive nerve fibres were detected in the PDL of the engrafted bio-hybrid implant (Fig. 3d). C-Fos immunoreactive neurons, which are detectable in the superficial layers of the medullary dorsal horn following noxious mechanical and chemical stimulation of the intraoral receptive fields, were dramatically increased in both the natural tooth and the bio-hybrid implant at 2 hours after orthodontic treatment (Fig. 3e). These results indicate that the engrafted bio-hybrid implant restored the ability to perceive noxious stimulation in cooperation with the maxillofacial region.

Regeneration of a vertical bone defect by transplantation of a bio-hybrid implant. The PDL plays an important role in maintaining the height and volume of the surrounding alveolar bone. Thus, tooth root fracture and periodontal disease are known to cause significant alveolar bone resorption[37]. Alveolar bone resorption resulting from dental diseases, which is often the most drastic in the buccal alveolar bone, makes it difficult to insert conventional dental implants without using bone regenerative approaches[38,39]. Finally, we investigated whether transplantation of the bio-hybrid implant could regenerate not only the functional periodontal tissue but also the surrounding alveolar bone of the recipient. To analyse alveolar bone regeneration after implantation, we developed a critical size bone defect model (3-wall bone defect model) that could not heal spontaneously in the murine lower jaw. The defects were prepared by extracting the lower first molar and then removing the buccal alveolar bone in the lower first molar region (Fig. 4a, b and Supplementary Fig. 6a). When the bio-hybrid implant was transplanted into this bone defect, vertical bone formation was observed from the marginal bone of the recipient at 14 days after transplantation, and the bone recovered almost completely with periodontal ligament space at 50 days after transplantation (Fig. 4c and Supplementary Fig. 6b). The regenerative bone area after transplantation of the bio-hybrid implant (Bio) significantly increased compared with a no transplant control (bone defect; BD) and a transplantation of osseo-integrated implant (OS) (BD; 57.9 $\pm$ 6.5%, OS; 45.5 $\pm$ 16.0%, Bio; 85.5 $\pm$ 10.7%, respectively; Fig. 4d, e). Clinically, the failure of dental implant therapy, including the loss or vertical subsidence of the implant after treatment, causes fundamental problems related to survival rates and subsequent dental treatment[40]. After transplantation of an osseo-integrated implant into the normal tooth loss region (OS), the subsidence of the implant was not observed between 0 and 50 days post-implantation (median: -0.04 mm, min: 0.00 mm, max: -0.05 mm). However, transplantation of the osseo-integrated implant into the 3-wall bone defect model (OS in BD) resulted in the dramatic subsidence of the implant (median: -0.69 mm, min: -0.25 mm, max: -0.75 mm; Fig. 4f, g). In contrast, after transplantation of the bio-hybrid implant into this bone defect model (Bio in BD), the subsidence of the implant was significantly prevented (median: -0.08 mm, min: 0.00 mm, max: -0.18 mm) compared with the osseo-integrated implants (Fig. 4f, g). These findings indicate that the PDL on the bio-hybrid implant regenerated the critical size bone defect and that the surrounding bone recognised the bio-hybrid implant as an artificial tooth that was equivalent to a natural tooth. Therefore, these results indicate that the bio-hybrid implant is a fibrous connective bio-hybrid organ that is fully functional *in vivo*.

Discussion

Here, we demonstrate the successful development of a bio-hybrid implant by using dental follicle stem cells to generate an artificial bio-hybrid organ with fibrous connective tissue (Fig. 5). This bio-hybrid implant restored physiological tooth functions, such as the ability to respond to mechanical stress and the ability to perceive noxious mechanical stimulation. The periodontal ligament present on the bio-hybrid implant also induced vertical bone recovery in a 3-wall bone defect model. This study demonstrates the potential for a next generation bio-hybrid implant for treating tooth loss.

Organs maintain the proper position and functionality *in vivo* through their connections to surrounding tissues via fibrous connective-tissues, including tendons, ligaments and muscles[9]. These fibrous connections contribute to biological mobility, such as eye and limb movements, and alleviate mechanical load by acting as shock absorbers[9]. The PDL, which is the connective fibre bundle penetrating into the cementum and alveolar bone[10], contributes to biological tooth functions, including the reduction of excessive occlusal loading and tooth movement, through bone remodelling[11,12]. Many dental implantology studies of tooth loss have attempted to restore periodontal tissue structure, *e.g.*, material-based approaches that were incorporated into the subsidence mechanism as a shock absorber[41], biochemical approaches coated by the PDL formation inducible peptide[42,43] and tissue engineering approaches using the periodontal ligament stem cells[17,18]. However, these technologies could not substitute and restore periodontal tissue functions[17,18]. In this study, the bio-hybrid implant connected to the surrounding alveolar bone through the periodontal tissues including the periodontal ligament with collagen fibre and cementum, but not osseo-integration, on the artificial dental implant surface. The bio-hybrid implant was responsive to mechanical stress through periodontal functions, including bone remodelling. These findings represent a significant advancement for the therapeutic concept of bio-hybrid artificial organs, as the biological fibrous connection achieved fully functional coalition of the artificial organ and living tissue.

The application of artificial organs for the substitution of dysfunctional organs, such as artificial eyes, cochlear implants and artificial arms, has been limited to a condition of peripheral nerves, muscles and bone, which can be sufficient to achieve biological activity at the dysfunctional site[5,6]. To regenerate damaged tissues around the transplantation site of artificial organ, bio-hybrid artificial organ therapy combined with tissue-derived stem cells and multipotent stem cells, including embryonic stem cells and induced pluripotent stem cells, in required[28]. Tooth loss due to root fracture or periodontal disease causes a large amount of alveolar bone resorption in the vertical and horizontal dimensions, and conventional dental therapies, including dental implant and autologous tooth trans-

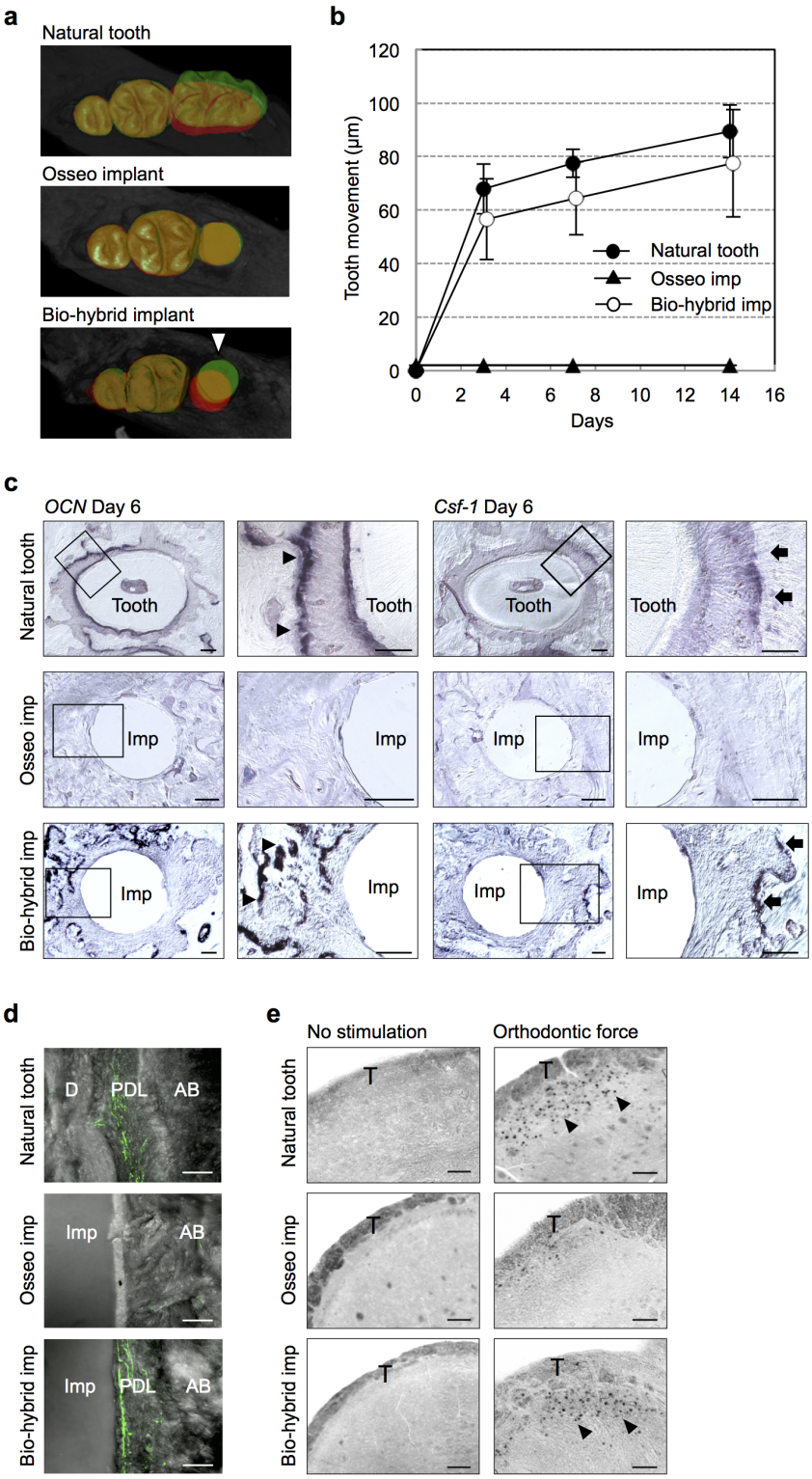

Figure 3 | Functional regeneration of a bio-hybrid implant. (a and b) Horizontal superposition of micro-CT images (*left*) of the natural tooth (*top*), osseo-integrated implant (*middle*) and bio-hybrid implant (*bottom*) at days 0 (red) and 14 days (green) of experimental orthodontic treatment. The movement distances of tooth and both implants by orthodontic force were measured after experimental orthodontic treatment at days 0, 3, 7 and 14 (*right*). Data represent the mean ± s.d.; $n = 5$ for natural tooth, osseo-integrated implant and bio-hybrid implant, respectively. (c) Sections of natural tooth, osseo-integrated and bio-hybrid implants were analysed by *in situ* hybridization analysis for *Ocn* and *Csf-1* mRNA at day 6 of orthodontic treatment. *Ocn* mRNA-positive cells (arrowhead) and *Csf-1* mRNA-positive cells (arrow) are indicated. Scale bar, 100 μm. (d) Nerve fibres in the PDL of the natural tooth (*top*), osseo-integrated implant (*middle*), and bio-hybrid implant (*bottom*) were analysed by immunohistochemistry using specific antibodies for neurofilament (NF; green). Scale bar, 50 μm. D, dentin; AB, alveolar bone; PDL, periodontal ligament; Imp, implant. (e) Analysis of c-Fos immunoreactive neurons in the medullary dorsal horns of mice after 0 hours (no stimulation, control; *left*) and 2 hours of stimulation by orthodontic force (*right*). c-Fos protein (arrowhead) was detectable after stimulation in the natural tooth (*top*) and bio-hybrid implant (*bottom*). Scale bar, 100 μm. T, spinal trigeminal tract.

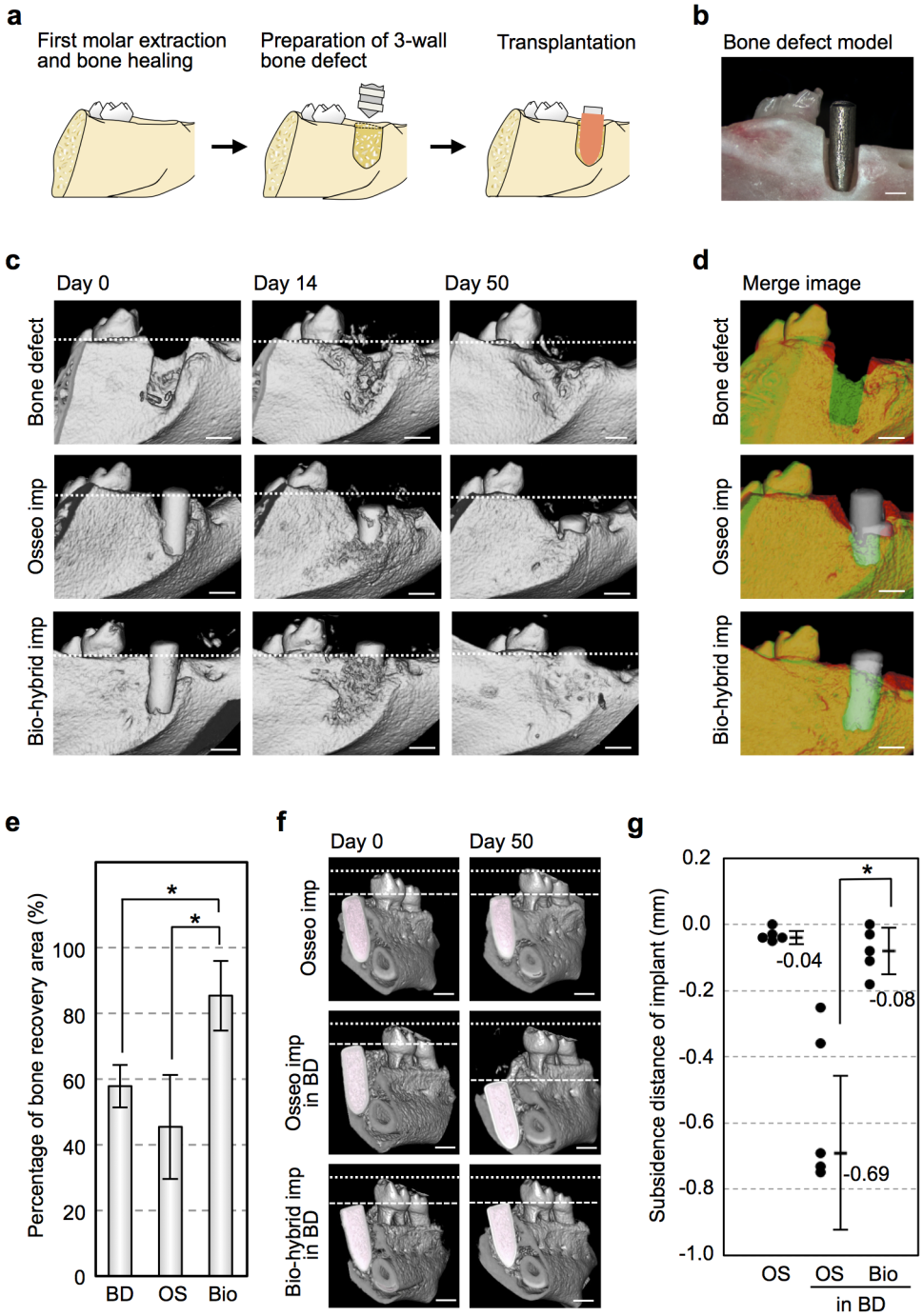

Figure 4 | Alveolar bone regeneration by transplantation of a bio-hybrid implant. (a) Schematic representation of the development of a murine 3-wall bone defect model and transplantation of the implant. (Drawings by C.T.) (b) Photographic representation of a murine 3-wall bone defect model and transplantation of the implant. Scale bar, 500 μm. (c) Micro-CT images of vertical alveolar bone regeneration processes in the bone defect without an implant (*top*), with transplantation of an osseo-integrated implant (*middle*) and with the transplantation of a bio-hybrid implant (*bottom*). Vertical bone formation was observed with the bio-hybrid implant, and the bone had recovered almost completely 50 days after transplantation. The superior edges of the recipient alveolar bone are indicated by a dotted line. Scale bar, 500 μm. (d) Three-dimensional superposition of micro-CT images for the non-treated control (*top*), the osseo-integrated implant (*middle*) and the bio-hybrid implant (*bottom*) in the 3-wall bone defect at 0 (red) and 50 days (green) after transplantation. Scale bar, 500 μm. (e) Regenerated bone area in the buccal region for the non-treated control (bone defect; BD), osseo-integrated implant (OS) and bio-hybrid implant (Bio) after 50 days in the 3-wall bone defect model. The data are presented as the mean ± s.d. with $n = 5$ for each experimental group. *$p < 0.01$ (Bonferroni test). (f) Three-dimensional frontal micro-CT images of the subsidence of the osseo-integrated implant into normal tooth loss region (*upper*), osseo-integrated implant into the bone defect model (*middle*) and bio-hybrid implant into the bone defect model (*lower*). The height to the top of the second molar cusp is indicated by the dotted line, and the top of the implant is marked by a dashed line. Scale bar, 500 μm. (g) Vertical subsidence of the osseo-integrated implants in the normal tooth loss region (OS) and in the 3-wall bone defect model (OS in BD) as well as the bio-hybrid implants in the 3-wall bone defect model (Bio in BD) 50 days after transplantation. The data are presented as the median ± s.d. with $n = 5$ for each experimental group. *$p < 0.01$ (Mann-Whitney U-test).

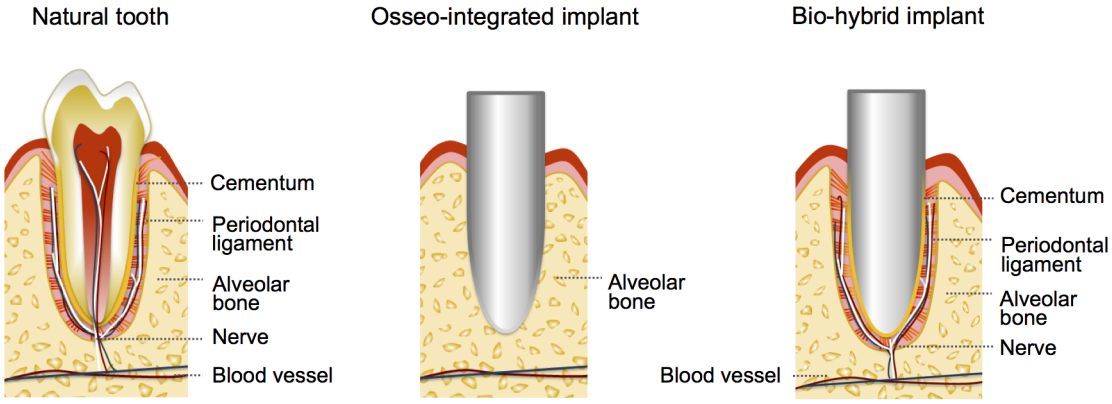

Figure 5 | Model of the connection to the periodontal tissues of a bio-hybrid implant. Schematic representation of the natural tooth, osseo-integrated implant and bio-hybrid implant. The bio-hybrid implant restored physiological functions, including bone remodelling, regeneration of severe bone-defect and responsiveness to noxious stimulations, through regeneration with periodontal tissues, such as cementum, PDL and alveolar bone. (Drawings by K.N.).

plantation, are difficult to apply to this clinical condition[37]. Although bone regenerative therapies have been attempted, including various utilisations of guided bone regeneration methods, autologous bone or cell transplantation and cytokine therapies[37,44], a clinical protocol for bone regeneration has not been available yet[36]. In this study, we demonstrated that a bio-hybrid implant induced vertical bone regeneration in a 3-wall bone defect model. These results suggest that the surrounding tissue, including alveolar bone, recognised the bio-hybrid implant as an equivalent organ to a natural tooth through its connection with the periodontal tissue on the surface of the titanium implant, which led to alveolar bone regeneration that was differentiated from the outer layer of dental follicle tissue after the transplantation. These findings indicate that transplantation of bio-hybrid artificial organs can achieve functional restoration and have the potential to restore the surrounding tissue via a mutual interaction between the bio-hybrid organ and the surrounding tissue.

Artificial organs with sensory functions, such as artificial eyes and cochlear implants, have been successfully used to restore visual and auditory functions via the proper afferent neurotransmission of external signals[5,6]. Furthermore, bio-hybrid artificial arms substituting arm locomotorium loss can reproduce arbitrary motions through efferent neurotransmission to an artificial machine[7]. Although these artificial therapies are effective and partially restore organ function, further technological improvements are required to exert biological organ functions via proper nerve innervations under the control of the CNS[5–7]. Teeth are peripheral target organs for the sensory trigeminal and sympathetic nerves, both of which play essential roles in tooth function and protection against noxious stimulations[12,34]. Current dental implant therapies are unable to receive the noxious stimulations due to a lack of interaction with the peripheral nerves and the periodontal tissue[15,16]. To recover the neuronal perception to mechanical forces, a next-generation bio-hybrid implant therapy that can fully restore the periodontal tissues is needed in the near future[11]. In the current study, we demonstrated that the successful innervation into the regenerated periodontal tissues around the bio-hybrid implant could restore responsiveness to noxious stimuli. These findings indicate that the transplantation of bio-hybrid artificial organ has great potential for the recovery of neuronal function via proper nerve innervations.

To realise future clinical applications of bio-hybrid implants, a suitable cell source must be identified. Current regenerative therapies for dental disorders have used stem cells derived from wisdom teeth/tooth germ tissue, such as the dental pulp, periodontal ligament, apical papillae and dental follicle, which have been shown to repair damaged tissues[45–48]. Currently, stem cells derived from the wisdom tooth (impacted third molar) germ of young patients, which can correspond to the ED18.5 dental follicle stem cells used here, are thought to be a potential candidate for periodontal tissue regeneration on a bio-hybrid implant[49,50]. The identification and the engineering optimisation of adult tissue stem cells useful for periodontal tissue regeneration will help develop a clinically relevant next-generation bio-hybrid implant therapy for treating tooth loss.

In conclusion, our study demonstrated a novel bio-hybrid implant with connected fibrous tissue as a bio-hybrid organ. This study represents a significant advancement in the development of a next-generation therapeutic for the treatment of tooth loss, as this bio-hybrid implant restored periodontal tissue structure and function through its fibrous tissue-based connection to the surrounding tissue.

Methods

Ethics statement of animal research. C57BL/6 and C57BL/6-TgN (act-EGFP) mice were purchased from SLC Inc., (Shizuoka, Japan). All handling and care of the mice conformed to the National Institute of Health (NIH) guidelines for animal research, and all experimental protocols involving animals were approved by the Tokyo University of Science Animal Care and Use Committee (Permit Number: N13010). All surgeries were performed under sodium pentobarbital anaesthesia, and all efforts were made to minimise suffering.

Tissue isolation and analysis of periodontal tissue formation. We extirpated the tooth germs at embryonic day (ED) 14.5, 18.5 and at postnatal day (PD) 7, and mature teeth were extracted at PD35. The isolated tooth germs were incubated in 50 U/ml dispase (BD, Franklin Lakes, NJ, USA) for 2 min at room temperature as a brief enzymatic treatment for the separation of the dental mesenchyme, or dental follicle tissue, from the tooth germ. After enzymatic treatment, the mesenchymal tissue and dental follicle tissues (DF) were separated using a fine needle in Dulbecco's modified Eagle's medium (D-MEM; Kohjin bio, Saitama, Japan) supplemented with 10% foetal calf serum (GIBCO, Grand Island, NY, USA), 100 U/mL penicillin (Sigma, St. Louis, MO, USA), 100 mg/mL streptomycin (Sigma) and 70 U/mL Deoxyribonuclease I from bovine pancreas (DNase I; Sigma). The periodontal ligament tissues were seceded from PD35 in the first molar using a surgical knife. Each of the isolated tissues were wrapped around hydroxyapatite particles (HA, CALCITITE; Hakuho, Tokyo, Japan) of approximately 50 μm in diameter. These HA particles were placed onto a cell culture insert (0.4 mm pore diameter; BD) and incubated at 37°C for 24 hours, and they were transplanted into a subrenal capsule for 30 days using syngeneic C57BL/6 mice (8 week-old, female) as the host.

***In situ* hybridization analysis.** *In situ* hybridisations were performed using 10 μm thick frozen sections. Digoxygenin-labelled probes for the specific transcripts were prepared by PCR using primers designed from published sequences (*F-spondin*, GenBank ID: NM_145584; *Periostin*, GenBank ID: NM_015784; *Osteocalcin* (*OCN*), GenBank ID: NM_007541; *Collagen type I* (*Col1*), GenBank ID: NM_007742; *Collagen type XVI alpha 1* (*Col16A*), GenBank ID: NM_028266; *Leprecan*, GenBank ID: NM_007541; *Nidogen-1* (*NID*), GenBank ID: NM_010917; *Scleraxis* (*Scx*), GenBank ID: NM_198885; *Tenascin-N* (*TNN*), GenBank ID: NM_177839; and *Colony-stimulating factor 1* (*Csf-1*), GenBank ID: NM_007778). The specific primers for these mouse genes were as follows: *F-spondin* (sense, 5′-AGACGGTCTACT-GGGCACTG-3′; antisense, 5′-TGCAAAAGGATGTGGT GGTA-3′), *Periostin* (sense, 5′-GGCTGAAGATGGTTCCTCTC-3′; antisense, 5′-CC ATGTGGCT-GTGTAAGGCATTC-3′), *OCN* (sense, 5′-AAGCCCAGCGACTCTGAGT CT-3′;

antisense, 5′-CCGGAGTCTATTCACCACCTTACT-3′), *Col1* (sense, 5′-CACT GCAAGAACAGCGTAGC-3′; antisense, 5′-TTGGTTTTTGGTCACGTTCA-3′), *Col16A* (sense, 5′-TACCTCCAGGATGCAGTTCC-3′; antisense, 5′-TCCTGTA-AGCTTTGG CCATT-3′), *Leprecan* (sense, 5′-GTCACAGGCTGAGAGGAAGG-3′; antisense, 5′-GC CCAGAGAAGAGTGTGTCC-3′), *NID* (sense, 5′-ACGTCA-TGGGAATCTTCAGC-3′; antisense, 5′-TGCAAACCGAACTTCTGATG-3′), *Scx* (sense, 5′-AAGAGGTGATGCC ACTAGTG-3′; antisense, 5′-TATACAAAAT-TTCCAGACTTTATATTATCAT-3′), *TNN* (sense, 5′-CAAGACCTGGAACA-GGGTGT-3′; antisense, 5′-TGCCTCTGTATTTCCCA ACC-3′), and *Csf-1* (sense, 5′-TACTGAACCTGCCTGCTGAA-3′; antisense, 5′-CC AGAGCTTGTGA-CAGGACA-3′). We superimposed images for *F-spondin*, *Periostin* and *OCN* staining using Adobe Photoshop software (Adobe Systems, San Jose, CA, USA).

Bio-hybrid implant fabrication and surface analysis. The implants were made of pure titanium wire (Nilaco, Tokyo, Japan) with a length of 1.7 mm and a diameter of 0.6 mm, and their apical sides were shaved into a conical shape. To promote cementum deposition around the implants, their surfaces were coated with HA, which is biocompatible and osteoinductive, via sputter deposition[32] (1–2 μm thickness of HA; Yamahachi dental MFG., Co., Aichi, Japan). DF tissues from ED18.5 mice were wrapped around the HA implants (5–6 tissues of each). The titanium and HA implants were coated with platinum, and their surfaces were observed using a S-4700 (Hitachi High-Tech, Tokyo, Japan) scanning electron microscope operated at 5 kV.

Transplantation of a bio-hybrid implant. The lower first molars of 4-week-old C57BL/6 mice were extracted under deep anaesthesia, and the resulting bone wounds were allowed to heal for 2–3 weeks. An incision of approximately 2.0 mm in length was made through the oral mucosa at the extraction site with a surgical knife to access the alveolar bone. A dental drill (NSK, Tochigi, Japan) and root canal files (MANI, Tochigi, Japan) were used to create a bony hole of approximately 0.8 mm in diameter and 1.3–1.5 mm in depth in the exposed alveolar bone surface. The HA and bio-hybrid implants were transplanted into the bony hole, and the incised oral mucosa was sutured with 8-0 nylon (Bear Medic, Chiba, Japan). To generate a critical size bone defect model (3-wall bone defect model) which could not heal spontaneously, the buccal supporting alveolar bone (0.7 mm in mesiodistal width and 1.5 mm in depth) in the lower first molar extracted region was removed using a dental drill under deep anaesthesia. The implants were transplanted into these defects using the same procedure described above.

Microcomputed tomography (Micro-CT). Radiographic imaging was performed by x-ray using a Micro-CT device (R_mCT; Rigaku, Tokyo, Japan) with exposure at 90 kV and 150 mA. Micro-CT images were captured using i-view R (Morita, Kyoto, Japan) and Imaris (Carl Zeiss, Oberkochen, Germany).

Histochemical analysis and immunohistochemistry. The tissues were excised and immersed in 10% formalin (Mildform 10 N; Wako, Osaka, Japan). After fixation, the tissues were decalcified in 10% sodium citrate and 22.5% formic acid for 3 days at 4°C. Tissue sections (5–8 μm) were made after embedding paraffin and were stained with either haematoxylin-eosin or azan. To visualise the elastic fibres, the sections were stained with a Resorcin-fuchsin solution (Muto Pure Chemicals, Tokyo, Japan) after 10% Oxone (Wako) treatment and then counterstained with 1% Orange G (Wako). The stained sections were observed using an Axioimager A1 microscope (Carl Zeiss) with an AxioCAM MRc5 (Carl Zeiss) camera. For fluorescent immunohistochemistry, 40 μm thick frozen sections were prepared and immunostained as previously described[35]. The sections were incubated with a primary antibody against the neurofilament SMI312 (1 : 1,000, mouse, Abcam, Cambridge, MA, USA). The primary antibody was detected using a highly cross-adsorbed Alexa Fluor® 594 Goat Anti-Rabbit IgG (H + L) (1 : 500, Life Technologies, Carlsbad, CA, USA). Fluorescence microscopy images were captured using a laser confocal microscope (LSM780; Carl Zeiss). To analyse the ability to perceive noxious stimulation by experimental orthodontic movement, we performed c-Fos immunohistochemistry as a pain response, which can be detected in the superficial layers of the medullary dorsal horn located in the brainstem[33,35]. The sections of the medullary dorsal horn in the brainstem region were incubated with anti-c-Fos Ab (1 : 10,000, Santa Cruz Biotechnology, Dallas, TX, USA). These sections were then immunostained with peroxidase-labelled goat anti-rabbit IgG (1 : 300, Cappel Laboratories, Cochranville PA, USA) and PAP immune complex (1 : 3,000, Cappel). The stained sections were observed on an Axiovert microscope (Carl Zeiss) equipped with an AxioCAM MRc5 camera (Carl Zeiss).

Electron microscopy and electron probe microanalysis. Each sample was fixed with 2.5% glutaraldehyde in 0.1 M phosphate buffer (pH 7.4) for 3 hours at 4°C. For SEM observations, samples were cut using a diamond disk and dehydrated in 100% ethanol. After coating with platinum, the samples were examined with a S-4700 SEM (Hitachi High-Tech) at 5 kV. For TEM analysis, the samples were post-fixed and embedded as a previously described[51]. Ultrathin sections were mounted on 150 mesh grids, stained with uranyl acetate and lead citrate and then examined by a H-7600 (Hitachi High-Tech) transmission electron microscope using an accelerating voltage of 75 kV. An electron probe microanalyzer (EPMA-1610; Shimadzu, Kyoto, Japan) was used for the elemental mapping of calcium (Ca), phosphorus (P), titanium (Ti), chlorine (Cl), magnesium (Mg), sodium (Na) and potassium (K). For the elemental analysis, undecalcified samples were embedded in epoxy resin and trimmed with diamond disks until the sagittal plane containing the centre of the implant was exposed. After polishing, the specimens were sputter-coated with carbon prior to elemental analysis.

Experimental orthodontic treatments. The orthodontic treatment was performed as described previously[33,35]. Experimental tooth movement was achieved with a horizontal orthodontic force of approximately 10–15 g that was applied continuously to the bio-hybrid implants of mice in the experimental group in the buccal direction using a dial tension gauge (Mitsutoyo, Kanagawa, Japan) for 3, 7 or 14 days. In the control group, the orthodontic force was applied in the buccal direction to the first molars of 7-week-old normal C57BL/6 mice in the same manner as the experimental group. Serial sections from day 6 samples were analysed by *in situ* hybridisation analysis for macrophage colony-stimulating factor-1 (*Csf-1*) and osteocalcin (*Ocn*) mRNA, as previously described[33,35]. The orthodontic movement distance of the bio-hybrid implants and natural first molars was measured using TRI/3D-BON software (Ratoc, Osaka, Japan).

Measurements of the regenerated bone area and subsidence distance of the implant. To evaluate the extent of alveolar bone regeneration in our buccal bone defect mouse model, we used a micro-CT device (Rigaku) to measure the alveolar bone area of the treated regions at 0 and 50 days post implantation. The area of the alveolar bone in the operated region was measured using Image J software (NIH, Bethesda, MD, USA). The alveolar bone area at day 50 was divided by the area at day 0 to calculate the regenerated bone area ratio. To analyse the subsidence of the implants in our buccal bone defect model, we measured the subsidence distance between the top of the second molar cusp and the top of the implant at 50 days post implantation. The vertical subsidence of implants is presented as the median ± standard deviation (s.d.).

Statistical analysis. Statistical significance was determined with a Bonferroni test and a Mann-Whitney *U*-test, and the data were analysed using the Common Gateway Interface Program (twk, Saint John's University).

1. Bengel, F. M. *et al.* Effect of sympathetic reinnervation on cardiac performance after heart transplantation. *N Engl J Med.* **345**, 731–738 (2001).
2. Copeland, J. G. *et al.* Cardiac Replacement with a Total Artificial Heart as a Bridge to Transplantation. *N Engl J Med.* **351**, 859–867 (2004).
3. Strain, A. J. & Neuberger, J. M. A bioartificial liver-state of the art. *Science* **295**, 1005–1009 (2002).
4. Davenport, A. *et al.* A wearable haemodialysis device for patients with end-stage renal failure: a pilot study. *Lancet* **370**, 2005–2010 (2005).
5. Kelly, S. K. *et al.* A hermetic wireless subretinal neurostimulator for vision prostheses. *IEEE Trans Biomed Eng.* **58**, 3195–3205 (2011).
6. Rauschecker, J. P. & Shannon, R. V. Sending Sound to the Brain. *Science* **295**, 1025–1029 (2002).
7. Kuiken, T. A. *et al.* Targeted reinnervation for enhanced prosthetic arm function. *Lancet* **369**, 371–380 (2007).
8. Huch, K. *et al.* Sports activities 5 years after total knee or hip arthroplasty: the Ulm Osteoarthritis Study. *Ann Rheum Dis.* **64**, 1715–1720 (2005).
9. Tomasek, J. J., Gabbiani, G., Hinz, B., Chaponnier, C. & Brown, R. A. Myofibroblasts and mechano-regulation of connective tissue remodeling. *Nat Rev Mol Cell Biol.* **3**, 349–363 (2002).
10. Avery, J. K. *Oral development and histology*. Steele, P. F. (ed.) 225–242 (Thieme Press, New York, 2002).
11. Shimono, M. *et al.* Regulatory mechanisms of periodontal regeneration. *Microsc Res Tech.* **60**, 491–502 (2003).
12. Proffit, W. R., Fields, H. W. & Sarver, D. M. *Contemporary orthodontics, 4th edition*. John, D. (ed.) 77–83 (Mosby Elsevier, St. Louis, 2006).
13. Rosenstiel, S. F., Land, M. F. & Fujimoto, J. *Contemporary fixed prosthodontics, 3rd edition*. John, S. & Penny, R. (ed.) 59–82 (Mosby, St. Louis, 2001).
14. Pokorny, P. H., Wiens, J. P. & Litvak, H. Occlusion for fixed prosthodontics: a historical perspective of the gnathological influence. *J Prosthet Dent.* **99**, 299–313 (2008).
15. Brenemark, P. I. & Zarb, G. A. *Tissue-integrated prostheses: osseointegration in clinical dentistry*. Albrektsson, T. (ed.) 211–232 (Quintessence Publishing Co, Inc, Chicago, 1985).
16. Burns, D. R., Beck, D. A. & Nelson, S. K. A review of selected dental literature on contemporary provisional fixed prosthodontic treatment: report of the Committee on Research in Fixed Prosthodontics of the Academy of Fixed Prosthodontics. *J Prosthet Dent.* **90**, 474–497 (2003).
17. Gault, P. *et al.* Tissue-engineered ligament: implant constructs for tooth replacement. *J Clin Periodontol.* **37**, 750–758 (2010).
18. Lin, Y. *et al.* Bioengineered periodontal tissue formed on titanium dental implants. *J Dent Res.* **90**, 251–256 (2011).
19. Ikeda, E. & Tsuji, T. Growing bioengineered teeth from single cells: potential for dental regenerative medicine. *Expert Opin Biol Ther.* **8**, 735–744 (2008).
20. Brockes, J. P. & Kumar, A. Appendage regeneration in adult vertebrates and implications for regenerative medicine. *Science* **310**, 1919–1923 (2005).
21. Segers, V. F. M. & Lee, R. T. Stem-cell therapy for cardiac disease. *Nature* **451**, 937–942 (2008).

22. Copelan, E. A. Hematopoietic stem-cell transplantation. *N Engl J Med.* **354**, 1813–1826 (2006).
23. Kim, J. H. *et al.* Dopamine neurons derived from embryonic stem cells function in an animal model of Parkinson's disease. *Nature* **418**, 50–56 (2002).
24. Elloumi-Hannachi, I., Yamato, M. & Okano, T. Cell sheet engineering: a unique nanotechnology for scaffold-free tissue reconstruction with clinical applications in regenerative medicine. *J Intern Med.* **267**, 54–70 (2010).
25. Sekine, H. *et al.* In vitro fabrication of functional three-dimensional tissues with perfusable blood vessels. *Nat Commun.* **4**, 1399 (2013).
26. Sasai, Y. Next-generation regenerative medicine: organogenesis from stem cells in 3D culture. *Cell stem cell* **12**, 520–530 (2013).
27. Silva, A. I., de Matos, A. N., Brons, I. G. & Mateus, M. An overview on the development of a bio-artificial pancreas as a treatment of insulin-dependent diabetes mellitus. *Med Res Rev.* **26**, 181–222 (2006).
28. Chen, W. *et al.* Restoration of auditory evoked responses by human ES-cell-derived otic progenitors. *Nature* **490**, 278–282 (2012).
29. Kitagawa, M., Ao, M., Miyauchi, M., Abiko, Y. & Takata, T. F-spondin regulates the differentiation of human cementoblast-like (HCEM) cells via BMP7 expression. *Biochem Biophys Res Commun.* **418**, 229–233 (2012).
30. Nishida, E. *et al.* Transcriptome database KK-Periome for periodontal ligament development: expression profiles of the extracellular matrix genes. *Gene* **404**, 70–79 (2007).
31. Thorfve, A. *et al.* Hydroxyapatite coating affects the Wnt signaling pathway during peri-implant healing *in vivo*. *Acta Biomater.* **10**, 1451–1462 (2014).
32. Ozeki, K., Yuhta, T., Fukui, Y., Aoki, H. & Nishimura, I. A functionally graded titanium/hydroxyapatite film obtained by sputtering. *J Mater Sci Mater Med.* **13**, 253–258 (2002).
33. Oshima, M. *et al.* Functional tooth regeneration using a bioengineered tooth unit as a mature organ replacement regenerative therapy. *PLoS One* **6**, e21531 (2011).
34. Dawson, P. E. *Functional occlusion: from TMJ to smile design*. John, D. (ed.) 18–26 (Mosby Elsevier, St. Louis, 2006).
35. Ikeda, E. *et al.* Fully functional bioengineered tooth replacement as an organ replacement therapy. *Proc Natl Acad Sci U S A.* **106**, 13475–13480 (2009).
36. Wise, G. E. & King, G. J. Mechanisms of Tooth Eruption and Orthodontic Tooth Movement. *J Dent Res.* **87**, 414–434 (2008).
37. Clementini, M., Morlupi, A., Canullo, L., Agrestini, C. & Barlattani, A. Success rate of dental implants inserted in horizontal and vertical guided bone regenerated areas: a systematic review. *Int J Oral Maxillofac Surg.* **41**, 847–852 (2012).
38. Araújo, M. G. & Lindhe, J. Dimensional ridge alterations following tooth extraction. An experimental study in the dog. *J Clin Periodontol.* **32**, 212–218 (2005).
39. Van der Weijden, F., Dell'Acqua, F. & Slot, D. E. Alveolar bone dimensional changes of post-extraction sockets in humans: a systematic review. *J Clin Periodontol.* **36**, 1048–1058 (2009).
40. Naert, I., Duyck, J. & Vandamme, K. Occlusal overload and bone/implant loss. *Clin Oral Implants Res.* **23**, 95–107 (2012).
41. Willer, J., Noack, N. & Hoffmann, J. Survival rate of IMZ implants: a prospective 10-year analysis. *J Oral Maxillofac Surg.* **61**, 691–695 (2003).
42. Kokubun, K., Kashiwagi, K., Yoshinari, M., Inoue, T. & Shiba, K. Motif-programmed artificial extracellular matrix. *Biomacromolecules* **9**, 3098–3105 (2008).
43. Yoshinari, M., Kato, T., Matsuzaka, K., Hayakawa, T. & Shiba, K. Prevention of biofilm formation on titanium surfaces modified with conjugated molecules comprised of antimicrobial and titanium-binding peptides. *Bio fouling.* **26**, 103–110 (2010).
44. Bueno, E. M. & Glowacki, J. Cell-free and cell-based approaches for bone regeneration. *Nat Rev Rheumatol.* **5**, 685–697 (2009).
45. Gronthos, S., Mankani, M., Brahim, J., Robey, P. G. & Shi, S. Postnatal human dental pulp stem cells (DPSCs) in vitro and in vivo. *Proc. Natl. Acad. Sci. U. S. A.* **97**, 13625–13630 (2000).
46. Seo, B. M. *et al.* Investigation of multipotent postnatal stem cells from human periodontal ligament. *Lancet* **364**, 149–155 (2004).
47. Sonoyama, W. *et al.* Characterization of the apical papilla and its residing stem cells from human immature permanent teeth: a pilot study. *J. Endod.* **34**, 166–171 (2008).
48. Huang, G. T., Gronthos, S. & Shi, S. Mesenchymal stem cells derived from dental tissues vs. those from other sources: their biology and role in regenerative medicine. *J. Dent. Res.* **88**, 792–806 (2009).
49. Kémoun, P. *et al.* Human dental follicle cells acquire cementoblast features under stimulation by BMP-2/-7 and enamel matrix derivatives (EMD) in vitro. *Cell Tissue Res.* **329**, 283–294 (2007).
50. Mehmet, E. *et al.* Comparison and optimisation of transfection of human dental follicle cells, a novel source of stem cells, with different chemical methods and electro-poration. *Neurochem Res.* **34**, 1272–1277 (2009).
51. Irie, T. *et al.* Intracellular transport of basement membrane-type heparan sulphate proteoglycan in adenoid cystic carcinoma cells of salivary gland origin: an immunoelectron microscopic study. *Virchows Arch.* **433**, 41–48 (1998).

Acknowledgments

We are grateful to Y. Shin and T. Takasu (Yamahachi Dental Mfg., Co., Aichi, Japan) for the hydroxyapatite coating of the dental implant. We also thank Y. Ochiai, N. Yamamoto and R. Koitabashi for their technical assistance. This work was supported by Organ Technologies Inc. We also received partial support from the Health and Labour Sciences Research Grants program from the Ministry of Health, Labour, and Welfare (No.21040101) to A.Y. (Tokyo Medical and Dental University) and a Grant-in-Aid for Scientific Research (A) from MEXT, Medicine, Dentistry and Pharmacy (No. 20249078) to T. Tsuji (2008–2010) from the Ministry of Education, Culture, Sports and Technology, Japan.

Author contributions

T. Tsuji and M. Oshima designed the research plan. M. Oshima, K.N., K.I., A.S., M.O. and T. Isobe performed the experiments. M. Oshima, T.T., S.K., T.T.-Y., T.I., M.S., K.T., T.K., A.Y. and T. Tsuji developed the new assay systems and wrote the discussion of the results. K.N., H.Y., C.T. and T.T. analysed the data. M. Oshima and T. Tsuji wrote the paper.

Additional information

Supplementary information accompanies this paper at http://www.nature.com/scientificreports

Competing financial interests: The authors declare no competing financial interests.

How to cite this article: Oshima, M. *et al.* Functional tooth restoration by next-generation bio-hybrid implant as a bio-hybrid artificial organ replacement therapy. *Sci. Rep.* **4**, 6044; DOI:10.1038/srep06044 (2014).